Electronic Supplementary Material (ESI) for ChemComm.

Remarkable Reactivity of a Rhodium(I) Boryl Complex Towards CO_2 and CS_2: Isolation of a Carbido Complex

Supporting Information

Sabrina I. Kalläne, Thomas Braun,* Michael Teltewskoi, Beatrice Braun, Roy Herrmann and Reik Laubenstein

Department of Chemistry, Humboldt-Universität zu Berlin, Brook-Taylor-Str. 2, 12489 Berlin, Germany
E-mail: thomas.braun@chemie.hu-berlin

General Methods

All reactions were carried out in an argon atmosphere. Benzene-d_6, toluene-d_8, cyclohexane-d_{12}, methylcyclohexane-d_{14}, cyclohexane, hexane, and hexamethyldisilane were dried by stirring over Na/K and then distilled. PFA (tetrafluoroethylen-perfluoroalkylvinylether copolymer) NMR tubes were used for highly sensitive compounds to inhibit reactions at glass surfaces. Complex $[Rh(Bpin)(PEt_3)_3]$ (**1**) was prepared according to the literature.[1,2] The NMR spectra were recorded at 300 K (if not stated otherwise) on a Bruker DPX 300 or a Bruker Avance III 300 NMR spectrometer. The ^1H NMR chemical shifts were referenced to residual benzene-d_5 at δ 7.16 ppm, toluene-d_7 at δ 2.09 ppm, cyclohexane-d_{11} at δ 1.43 ppm or methylcyclohexane-d_{13} at δ 1.62 ppm. The $^{13}C\{^1H\}$ NMR chemical shifts were referenced to benzene-d_6 at δ 128.06 ppm, to toluene-d_8 at δ 20.43 ppm, to cyclohexane-d_{12} at δ 27.23 ppm, and to methylcyclohexane-d_{14} at δ 35.37 ppm. The $^{11}B\{^1H\}$ NMR spectra were referenced to external $BF_3{\cdot}OEt_2$ at δ 0.0 ppm, and the $^{31}P\{^1H\}$ NMR spectra to external H_3PO_4 at δ 0.0 ppm. In order to get a ^2H lock signal, benzene-d_6 was introduced in the space between the glass NMR tubes and the PFA inliners, which contained the reaction mixture with hexamethyldisilane or cyclohexane as a solvent. GC-MS spectra were measured at an Agilent 6890N gas-phase chromatograph (Agilent 19091S-433 Hewlett-Packard) which was equipped with an Agilent 5973 Network mass selective detector at 70 eV. Microanalyses were performed with a HEKAtech Euro EA Elemental Analyzer. Mass spectra were measured with a Micromass Q-Tof-2 instrument equipped with a Linden LIFDI source (Linden CMS GmbH). Infrared spectra were recorded with a Bruker Vertex 70 spectrometer equipped with an ATR unit (diamond) and Raman spectra were recorded with a Bruker Vertex 70 with RAM II (Nd:YAG-Laser; 1064 nm).

Treatment of [Rh(Bpin)(PEt$_3$)$_3$] (1) with CO$_2$: Formation of *trans*-[Rh(OBpin)(CO)(PEt$_3$)$_2$] (2)

A solution of [Rh(Bpin)(PEt$_3$)$_3$] (**1**) (31.0 mg, 53 μmol) in cyclohexane (0.2 mL) in a Young NMR tube equipped with a PFA tube was cooled to 77 K, degassed and pressurized with CO$_2$ to 1 atm. The orange-red reaction solution turned light yellow. After 1 h at room temperature the NMR spectroscopic data of the reaction solution revealed the complete conversion of **1** and the formation of *trans*-[Rh(OBpin)(CO)(PEt$_3$)$_2$] (**2**) and PEt$_3$. The reaction solution always contained small amounts (5%) of [Rh(H)(CO)(PEt$_3$)$_3$],[3] which was identified by comparison of the NMR and IR data with these in the literature. Analytical data for *trans*-[Rh(OBpin)(CO)(PEt$_3$)$_2$] (**2**): ^{1}H NMR (300.1 MHz, toluene-d$_8$, 203 K): *δ* 1.75-1.40 (br m, CH$_2$, CH$_3$), the signals of the phosphine ligands are superimposed by the signals of free PEt$_3$; ^{11}B{^{1}H}NMR (96.3 MHz, toluene-d$_8$): *δ* 21.0 (s); ^{13}C{^{1}H} NMR (75.5 MHz, toluene-d$_8$, 223 K): *δ* 192.1 (d, $J_{\mathrm{Rh,C}}$ = 67 Hz, CO), 78.8 (s, *C*(CH$_3$)$_2$), 25.7 (s, C(*C*H$_3$)$_2$), ~16 (br s, CH$_2$), 8.9 (br s, CH$_3$); ^{31}P{^{1}H} NMR (121.5 MHz, toluene-d$_8$): *δ* 28-22 (br); ^{31}P{^{1}H} NMR (121.5 MHz, toluene-d$_8$, 263 K): *δ* 24.7 (br d, $J_{\mathrm{Rh,P}} \approx$ 120 Hz, **2**), -20.8 (br s, PEt$_3$); ^{31}P{^{1}H} NMR (121.5 MHz, toluene-d$_8$, 203 K): *δ* 24.5 (d, $J_{\mathrm{Rh,P}}$ = 124 Hz, **2**), -22.1 (br s, PEt$_3$); IR (ATR): $\tilde{\nu}$ 1941 (C≡O) cm^{-1}. Complex **2′** was prepared in a similar manner using ^{13}CO$_2$. Selected analytical data for *trans*-[Rh(OBpin)(^{13}CO)(PEt$_3$)$_2$] (**2′**): ^{31}P{^{1}H} NMR (121.5 MHz, toluene-d$_8$, 203 K): *δ* 24.5 (d, $J_{\mathrm{Rh,P}}$ = 124 Hz, **2′**); ^{31}P{^{1}H} NMR (121.5 MHz, toluene-d$_8$, 183 K): *δ* 24.5 (dd, $J_{\mathrm{Rh,P}}$ = 124 Hz, $J_{\mathrm{C,P}}$ = 15 Hz); IR (ATR): $\tilde{\nu}$ 1896 (^{13}C≡O) cm^{-1}.

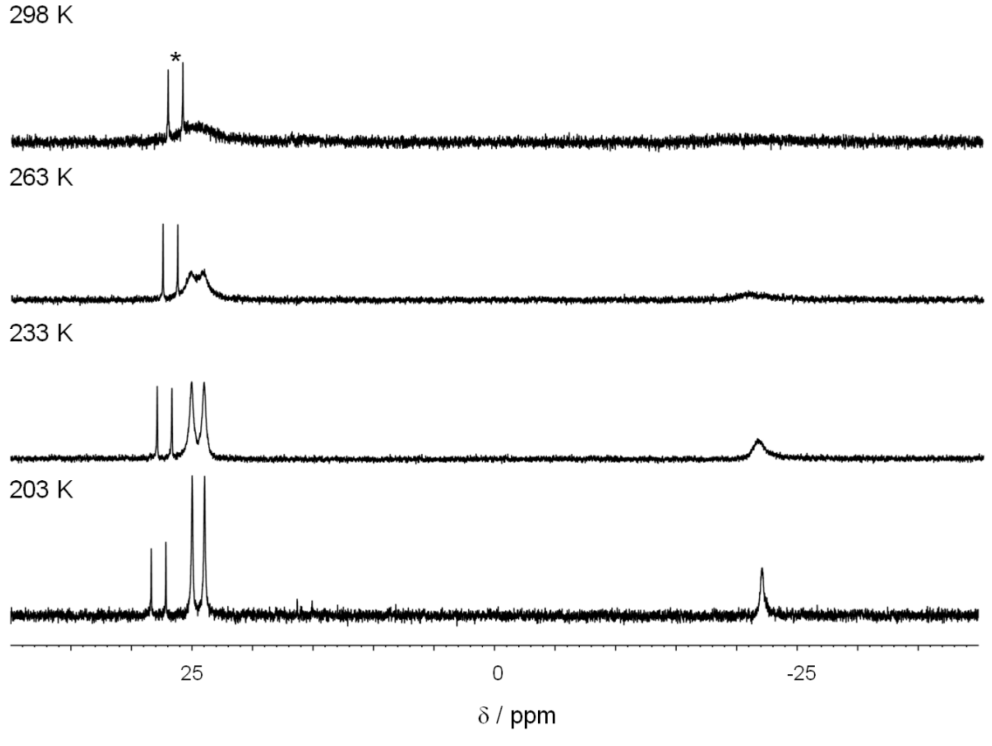

Figure S1. Variable temperature ^{31}P{^{1}H} NMR spectra (121.5 MHz, toluene-d$_8$) of a solution of complex **2** and free PEt$_3$ (*: small amounts of [Rh(H)(CO)(PEt$_3$)$_3$]).

Yellow crystals of *trans*-[Rh(OBpin)(CO)(PEt_3)$_2$]·HOBpin (**2**·**HOBpin**) were obtained at –30 °C after six months by crystallization from a solution of the reaction products in *n*-hexane. Analytical data for *trans*-[Rh(OBpin)(CO)(PEt_3)$_2$]·HOBpin (**2**·**HOBpin**): ^{1}H NMR (300.1 MHz, benzene-d$_6$): δ 6.08 (s, 1H, OH), 1.74 (br m, 12H, CH_2), 1.23 (br m, 24H, CH_3), 1.20-1.00 (br m, 18H, CH_3); ^{11}B{^{1}H} NMR (96.3 MHz, benzene-d$_6$): δ 22.4 (s), 21.6 (s); ^{13}C{^{1}H} NMR (75.5 MHz, benzene-d$_6$): δ 82.1 (s, *C*(CH_3)$_2$), 79.2 (s, *C*(CH_3)$_2$), 25.4 (s, C(*C*H$_3$)$_2$), 24.7 (s, C(*C*H$_3$)$_2$), 16.5 (t, *J* = 13 Hz, CH_2), 8.6 (s, CH_3), the signal for the Rh-CO carbon atom was not observed; ^{31}P{^{1}H} NMR (121.5 MHz, benzene-d$_6$): δ 24.7 (d, $J_{Rh,P}$ = 125 Hz).

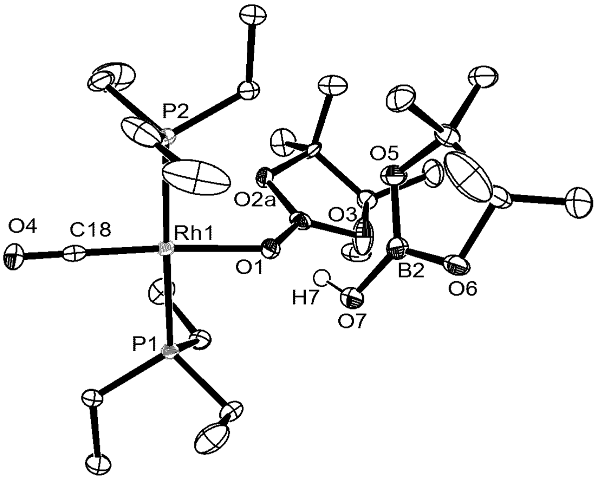

Figure S2. An ORTEP diagram of *trans*-[Rh(OBpin)(CO)(PEt_3)$_2$]·HOBpin (**2**·**HOBpin**). The ellipsoids are drawn at the 50% probability level. The hydrogen atoms are omitted for clarity.

Table S1. Selected distances (Å) and angles (°) for **2**·**HOBpin** with estimated standard deviations in parentheses

bond/ distance	length	bond	angle
Rh1-C18	1.7948(17)	C18-Rh1-O1	176.13(6)
Rh1-O1	2.0638(11)	C18-Rh1-P1	93.63(5)
Rh1-P1	2.3150(4)	O1-Rh1-P1	84.11(3)
Rh1-P2	2.3224(4)	C18-Rh1-P2	88.70(5)
O1-B1	1.324(2)	O1-Rh1-P2	93.68(3)
O3-B1	1.382(2)	P1-Rh1-P2	176.838(15)
O2a-B1	1.308(9)	B1-O1-Rh1	126.69(11)
O2b-B1	1.492(7)	O4-C18-Rh1	179.09(15)
O5-B2	1.378(2)		
O6-B2	1.379(2)		
O7-B2	1.337(2)		
O4-C18	1.157(2)		
O1-O7	2.658(2)		

Treatment of [Rh(Bpin)(PEt_3)$_3$] (1) with CO: Formation of *cis*-[Rh(Bpin)(CO)(PEt_3)$_2$] (3)

A solution of [Rh(Bpin)(PEt_3)$_3$] (**1**) (33.4 mg, 57 µmol) in methylcyclohexane-d_{14} (0.3 mL) in a Young NMR tube equipped with a PFA tube was cooled to 77 K, degassed and pressurized with CO to 1 atm. The orange-red reaction solution turned light yellow. After 15 min at room temperature the $^{31}P\{^1H\}$ NMR spectroscopic data of the reaction solution revealed the complete conversion of **1** and the quantitative formation of *cis*-[Rh(Bpin)(CO)(PEt_3)$_2$] (**3**) and PEt_3. Analytical data for *cis*-[Rh(Bpin)(CO)(PEt_3)$_2$] (**3**): ^1H NMR (300.1 MHz, methylcyclohexane-d_{14}): δ 2.04 (m, q in the $^1H\{^{31}P\}$ NMR spectrum, 12H, $J_{H,H}$ = 7 Hz, CH_2), 1.60 (s, 12H, CH_3), 1.47 (m, t in the $^1H\{^{31}P\}$ NMR spectrum, 18H, $J_{H,H}$ = 8 Hz, CH_3); $^{11}B\{^1H\}$NMR (96.3 MHz, methylcyclohexane-d_{14}): δ 42 (br s); $^{13}C\{^1H\}$ NMR (75.5 MHz, methylcyclohexane-d_{14}): δ 200.8 (dt, $J_{Rh,C}$ = 69 Hz, $J_{P,C}$ = 3 Hz, CO), 82.5 (s, $C(CH_3)_2$), 26.1 (s, $C(CH_3)_2$), 22.5 (t, J = 10 Hz, CH_2), 8.7 (br s, CH_3); $^{31}P\{^1H\}$ NMR (121.5 MHz, methylcyclohexane-d_{14}): δ 17.0 (d, $J_{Rh,P}$ = 110 Hz); $^{31}P\{^1H\}$ NMR (121.5 MHz, methylcyclohexane-d_{14}, 183 K): δ 21.1 (dd, $J_{Rh,P}$ = 81 Hz, $J_{P,P}$ = 36 Hz), 15.1 (dd, $J_{Rh,P}$ = 135 Hz, $J_{P,P}$ = 36 Hz); Raman (*n*-hexane): $\tilde{\nu}$ 1985 (C≡O), 1935 (C≡O) cm^{-1}; MS (LIFDI, Me_6Si_2): *m/z* 494 $[M]^+$, 466 $[M\text{-}CO]^+$. Complex **3′** was prepared in a similar manner using ^{13}CO. Selected analytical data for [Rh(Bpin)(CO)(PEt_3)$_2$] (**3′**): Raman (*n*-hexane): $\tilde{\nu}$ 1938 (C≡O), 1885 (C≡O) cm^{-1}.

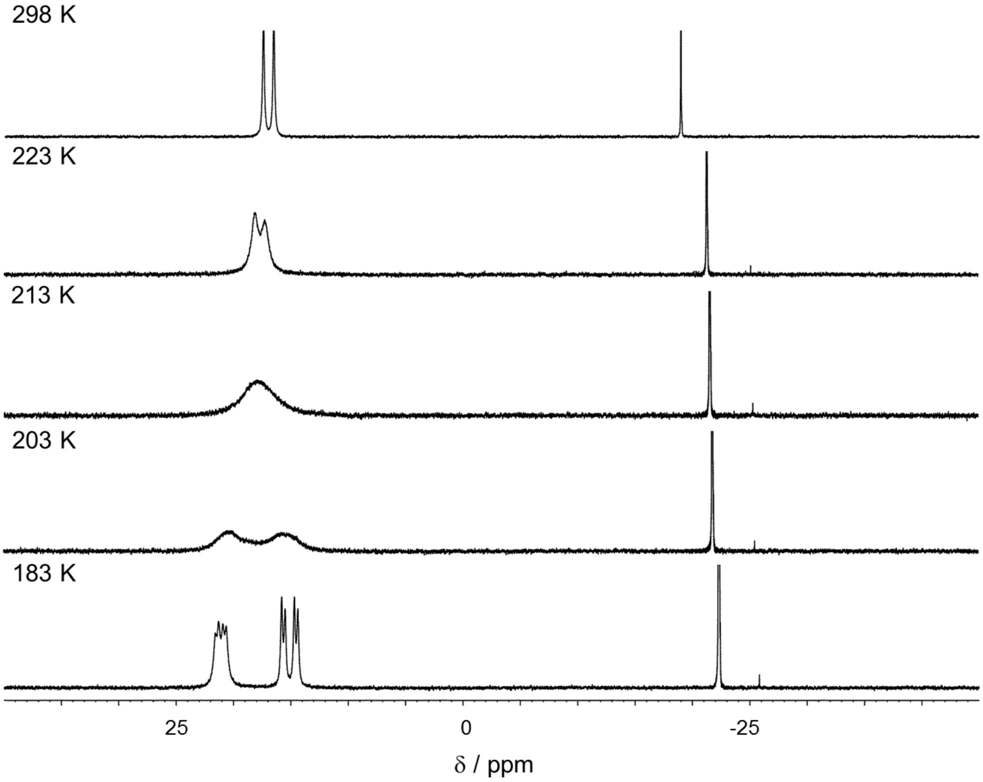

Figure S3. Variable temperature $^{31}P\{^1H\}$ NMR spectra (121.5 MHz, methylcyclohexane-d_{14}) of a solution of complex **3** and free PEt_3.

Treatment of *trans*-[Rh(OBpin)(CO)(PEt$_3$)$_2$] (2) with B$_2$pin$_2$: Formation of *cis*-[Rh(Bpin)(CO)(PEt$_3$)$_2$] (3)

A solution of *trans*-[Rh(OBpin)(CO)(PEt$_3$)$_2$] (**2**) and PEt$_3$ was prepared from [Rh(Bpin)(PEt$_3$)$_3$] (**1**) (26.3 mg, 57 µmol) and CO$_2$ in methylcyclohexane (0.2 mL) in a Young NMR tube equipped with a PFA tube. The reaction mixture was then treated with B$_2$pin$_2$ (14.5 mg, 57 µmol) in methylcyclohexane (0.1 mL). After 2 d at room temperature the NMR spectroscopic data of the reaction solution revealed the complete conversion of **2** and the formation of *cis*-[Rh(Bpin)(CO)(PEt$_3$)$_2$] (**3**). Complex **3′** was prepared in a similar manner starting from **2′**.

Treatment of [Rh(Bpin)(PEt$_3$)$_3$] (1) with N$_2$O: Synthesis of [Rh(OBpin)(PEt$_3$)$_3$] (4)

A slow stream of N$_2$O was passed for 20 s through a solution of [Rh(Bpin)(PEt$_3$)$_3$] (**1**) (146 mg, 0.25 mmol) in Me$_6$Si$_2$ (0.5 mL) in a Schlenk flask equipped with a PFA tube. The volatiles were removed under vacuum and the residue was dissolved in *n*-hexane (0.3 mL). After cooling the solution to 203 K an orange solid precipitated, which was separated, washed with *n*-hexane (3 x 0.15 mL) and dried in vacuum. Yield: 116 mg (77%). Compound **4** was identified by comparison of the NMR data with these in the literature.[4]

Yellow crystals of [Rh(OBpin)(PEt$_3$)$_3$] (**4**) were grown at –30 °C from a *n*-hexane solution.

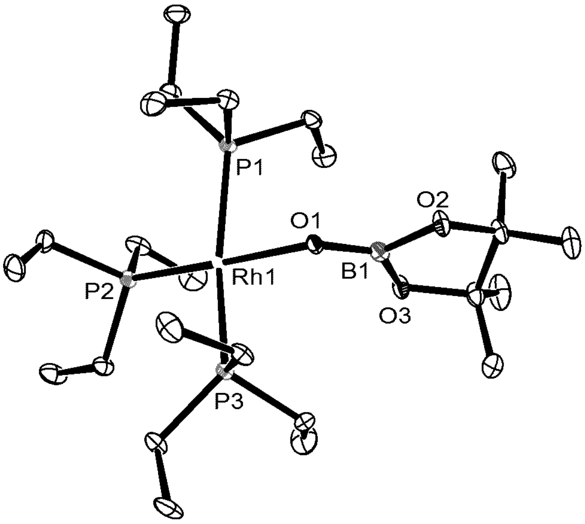

Figure S4. An ORTEP diagram of [Rh(OBpin)(PEt$_3$)$_3$]·(**4**). The ellipsoids are drawn at the 50% probability level. The hydrogen atoms are omitted for clarity.

Table S2. Selected bond lengths (Å) and angles (°) for **4** with estimated standard deviations in parentheses

bond	length	bond	angle
Rh1-O1	2.109(2)	O1-Rh1-P2	174.53(6)
Rh1-P1	2.3141(8)	O1-Rh1-P3	81.82(6)
Rh1-P2	2.1968(8)	P2-Rh1-P3	101.69(3)
Rh1-P3	2.3095(7)	O1-Rh1-P1	80.52(6)
O1-B1	1.304(4)	P1-Rh1-P2	97.04(3)
O2-B1	1.416(4)	P1-Rh1-P3	157.47(3)
O3-B1	1.411(4)	B1-O1-Rh1	131.0(2)
		O1-B1-O3	127.8(3)
		O1-B1-O2	123.2(3)
		O2-B1-O3	109.0(3)

Treatment of [Rh(OBpin)(PEt$_3$)$_3$] (4) with CO

A solution of [Rh(OBpin)(PEt$_3$)$_3$] (**4**) (15.0 mg, 25 μmol) in toluene-d$_8$ (0.2 mL) in a Young NMR tube equipped with a PFA tube was cooled to 77 K, degassed and pressurized with CO to 1 atm. After 1 h at room temperature the ^{31}P{^{1}H} NMR spectroscopic data of the reaction solution revealed that **4** was converted into *trans*-[Rh(OBpin)(CO)(PEt$_3$)$_2$] (**2**) in 20% yield (according to the ^{31}P{^{1}H} NMR spectrum at 203 K).

Treatment of [Rh(OBpin)(PEt$_3$)$_3$] (4) with B$_2$pin$_2$

A solution of [Rh(OBpin)(PEt$_3$)$_3$] (**4**) (11.4 mg, 19 μmol) in cyclohexane (0.2 mL) in a NMR tube was treated with B$_2$pin$_2$ (4.8 mg, 19 μmol). After 1 d the ^{31}P{^{1}H} NMR spectroscopic data of the reaction solution revealed the complete conversion of **4** and the quantitative formation of [Rh(Bpin)(PEt$_3$)$_3$] (**1**). The formation of pinBOBpin was confirmed by ^{11}B{^{1}H} NMR spectroscopy and GC-MS analysis.

Treatment of [Rh(Bpin)(PEt$_3$)$_3$] (1) with PhNCO: Formation of *trans*-[Rh{N(Ph)Bpin}(CO)(PEt$_3$)$_2$] (5)

a) A solution of [Rh(Bpin)(PEt$_3$)$_3$] (**1**) (31.5 mg, 54 μmol) in Me$_6$Si$_2$ (0.2 mL) in a NMR tube equipped with a PFA tube was treated with PhNCO (5.8 μL, 54 μmol). Immediately the orange-red reaction solution turned light yellow. After 5 min at room temperature the ^{31}P{^{1}H} NMR spectroscopic data of the reaction solution revealed the complete conversion of **1** and the formation of *trans*-

$[Rh\{N(Ph)Bpin\}(CO)(PEt_3)_2]$ (**5**) in 90% yield as well as the formation of PEt_3. Analytical data for *trans*-$[Rh\{N(Ph)Bpin\}(CO)(PEt_3)_2]$ (**5**): ^1H NMR (300.1 MHz, benzene-d_6): δ 7.96 (d, 2H, $J_{H,H}$ = 8 Hz, CH_{ar}), 7.19 (t, 2H, $J_{H,H}$ = 8 Hz, CH_{ar}), 6.90 (t, 1H, $J_{H,H}$ = 8 Hz, CH_{ar}), 1.66 (m, 6H, CH_2), 1.53 (m, 6H, CH_2), 1.17 (s, 12H, CH_3), 1.00 (t, 18H, $J_{H,H}$ = 8 Hz, CH_3); $^{11}B\{^1H\}$ NMR (96.3 MHz, Me_6Si_2): δ 24.3 (s); $^{13}C\{^1H\}$ NMR (75.5 MHz, benzene-d_6): δ 192.5 (dt, $J_{Rh,C}$ = 67 Hz, $J_{P,C}$ = 17 Hz, CO), 158.0 (s, NC_{ar}), 127.9 (s, CH_{ar}), 123.5 (s, CH_{ar}), 115.9 (s, CH_{ar}), 80.1 (s, $C(CH_3)_2$), 25.4 (s, $C(CH_3)_2$), 16.8 (t, J = 12 Hz, CH_2), 8.5 (s, CH_3); $^{31}P\{^1H\}$ NMR (121.5 MHz, Me_6Si_2): δ 21.8 (d, $J_{Rh,P}$ = 132 Hz); IR (ATR): $\tilde{\nu}$ 1944 (C≡O) cm^{-1}.

b) A solution of $[Rh(Bpin)(PEt_3)_3]$ (**1**) (31.5 mg, 54 µmol) in toluene-d_8 (0.25 mL) in a NMR tube equipped with a PFA tube was treated with PhNCO (5.8 µL, 54 µmol) at 203 K. The reaction was monitored by NMR spectroscopy and slowly warmed up to room temperature. Between 213 K and 233 K the $^{31}P\{^1H\}$ NMR spectroscopic data revealed the presence of an intermediate. Analytical data for the intermediate: $^{31}P\{^1H\}$ NMR (121.5 MHz, toluene-d_8): δ 24.8 (dt, 1P, $J_{Rh,P}$ = 111 Hz, $J_{P,P}$ = 40 Hz, P_{trans}), 17.1 (dd, 2P, $J_{Rh,P}$ = 150 Hz, $J_{P,P}$ = 40 Hz, P_{cis}).

Yellow crystals of *trans*-$[Rh\{N(Ph)Bpin\}(CO)(PEt_3)_2]$ (**5**) were grown at -30 °C from a *n*-hexane solution.

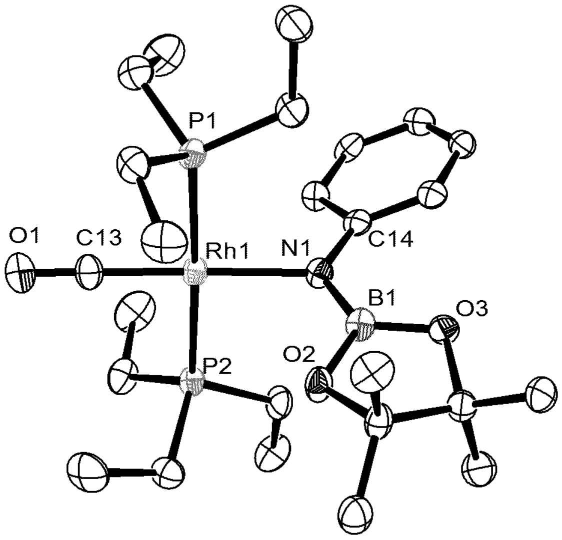

Figure S5. An ORTEP diagram of *trans*-$[Rh\{N(Ph)Bpin\}(CO)(PEt_3)_2]$ (**5**). The ellipsoids are drawn at the 50% probability level. The hydrogen atoms are omitted for clarity. The asymmetric unit cell contains two crystallographically independent molecules; only one of them is shown.

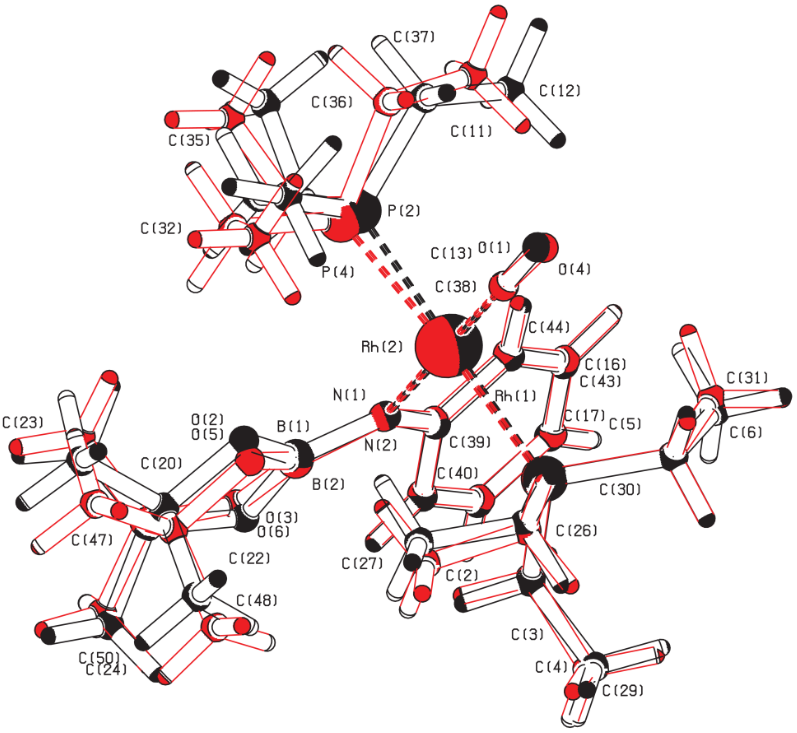

Figure S6. Overlay plot of both independent moleculesof *trans*-[Rh{N(Ph)Bpin}(CO)(PEt$_3$)$_2$] (**5**) using AutoMolFit implemented in PLATON. The two independent molecules of **5** in the asymmetric unit show slightly different conformations. Despite the rare occurrence of the space group P1 (see Table S5), an inversion symmetric structure is excluded.

Table S3. Selected bond lengths (Å) and angles (°) for **5** with estimated standard deviations in parentheses (the data for the second crystallographically independent molecules are comparable and are therefore not shown)

bond	length	bond	angle
Rh1-C13	1.797(6)	C13-Rh1-N1	178.7(2)
Rh1-N1	2.114(4)	C13-Rh1-P1	89.2(2)
Rh1-P1	2.3284(14)	N1-Rh1-P1	91.23(13)
Rh1-P2	2.3128(15)	C13-Rh1-P2	88.4(2)
N1-B1	1.399(8)	N1-Rh1-P2	91.22(13)
O2-B1	1.409(8)	P1-Rh1-P2	177.28(6)
O3-B1	1.394(7)	B1-N1-Rh1	117.9(4)
C13-O1	1.162(7)	O1-C13-Rh1	179.5(6)
N1-C14	1.398(7)	B1-N1-C14	122.4(5)
		Rh1-N1-C14	119.5(3)

Treatment of [Rh(Bpin)(PEt_3)$_3$] (1) with 1 eq. CS_2: Formation of [Rh(SBpin)(CS)(PEt_3)$_x$] (x = 2,3) (6)

A solution of CS_2 (2.5 µL, 41 µmol) in cyclohexane (0.05 mL) was added to a solution of [Rh(Bpin)(PEt_3)$_3$] (**1**) (23.9 mg, 41 µmol) in cyclohexane (0.3 mL) in a PFA tube. After 5 min at room temperature the $^{31}P\{^1H\}$ NMR spectroscopic data of the reaction solution revealed the complete conversion of **1** and the quantitative formation of [Rh(SBpin)(CS)(PEt_3)$_x$] (x = 2,3) (**6**). Analytical data for the solution of [Rh(SBpin)(CS)(PEt_3)$_2$] (x = 2,3) (**6**): $^{11}B\{^1H\}$ NMR (96.3 MHz, Me_6Si_2): δ 34.0 (s); $^{13}C\{^1H\}$ NMR (75.5 MHz, Me_6Si_2): δ 277.7 (br d, $J_{\mathrm{Rh,C}}$ = 67 Hz, CS), 82.5 (s, $\mathit{C}(CH_3)_2$), 25.9 (s, $C(\mathit{C}H_3)_2$), 18.4 (br s, CH_2), 9.9 (s, CH_3); $^{31}P\{^1H\}$ NMR (121.5 MHz, methylcyclohexane-d$_{14}$): δ ~5 (br s); $^{31}P\{^1H\}$ NMR (121.5 MHz, methylcyclohexane-d$_{14}$, 193 K): δ ~14 (br s); $^{31}P\{^1H\}$ NMR (121.5 MHz, toluene-d$_8$, 203 K): δ ~16 (br s); IR (ATR): $\tilde{\nu}$ 1280 (C≡S) cm^{-1}; MS (LIFDI, Me_6Si_2): *m/z* 542 [M]$^+$. Complex **6´** was prepared in a similar manner using $^{13}CS_2$. Selected analytical data for *trans*-[Rh(SBpin)(^{13}CS)(PEt_3)$_2$] (**6´**): IR (ATR): $\tilde{\nu}$ 1227 (^{13}C≡S) cm^{-1}.

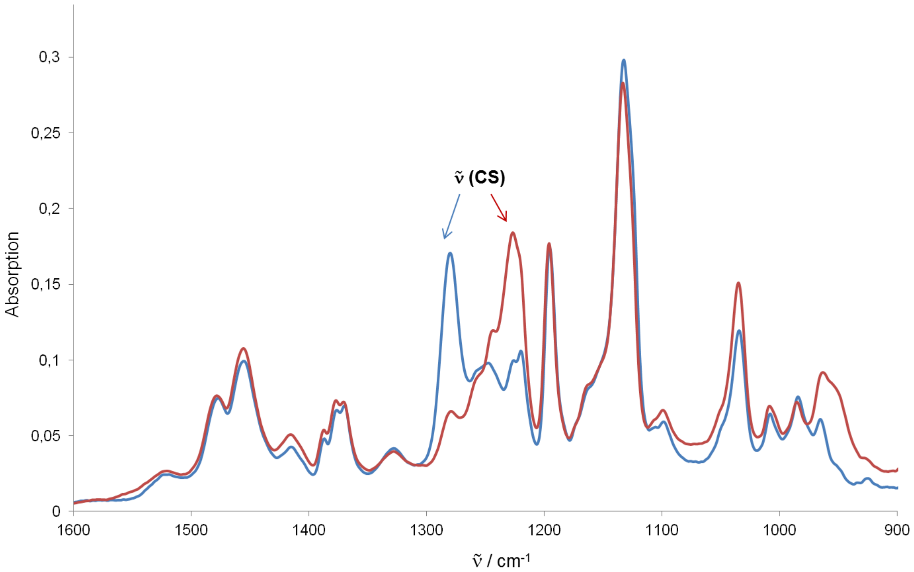

Figure S7. Part of the IR spectra of the solution after the reaction of [Rh(Bpin)(PEt_3)$_3$] (**1**) with CS_2 (blue line) or $^{13}CS_2$ (red line).

Treatment of [Rh(Bpin)(PEt_3)$_3$] (1) with 0.5 eq. CS_2: Synthesis of *trans*-[Rh$_2$(µ-C)(SBpin)$_2$(PEt_3)$_4$] (7)

A solution of CS_2 (5.8 µL, 95 µmol) in cyclohexane (0.1 mL) was added to a solution of [Rh(Bpin)(PEt_3)$_3$] (**1**) (111.5 mg, 191 µmol) in cyclohexane (0.3 mL) in a PFA tube. After 5 min at room temperature an orange solid precipitated, which was separated, washed with *n*-hexane (2 x 0.1 mL) and dried in vacuum. Yield: 69 mg (72%). Analytical data for *trans*-[Rh$_2$(µ-C)(SBpin)$_2$(PEt_3)$_4$]

(**7**): Anal. Calcd. (%) for $C_{37}H_{84}B_2O_4P_4Rh_2S_2$: C, 44.06; H, 8.40; S, 6.38. Found: C, 44.06; H, 8.66; S, 5.74; ^{1}H NMR (300.1 MHz, benzene-d$_6$): δ 2.19 (m, q in the ^{1}H{^{31}P} NMR spectrum, 24H, $J_{H,H}$ = 8 Hz, CH$_2$), 1.19 (m, t in the ^{1}H{^{31}P} NMR spectrum, 36H, $J_{H,H}$ = 8 Hz, CH$_3$), 1.17 (s, 24H, CH$_3$); ^{11}B{^{1}H}NMR (96.3 MHz, benzene-d$_6$): δ 33.6 (s); ^{13}C{^{1}H} NMR (75.5 MHz, cyclohexane-d$_{12}$): δ 439.4 (tquin, $J_{Rh,C}$ = 45 Hz, $J_{P,C}$ = 11 Hz, RhCRh), 81.7 (s, *C*(CH$_3$)$_2$), 25.1 (s, C(*C*H$_3$)$_2$), 17.1 (t, J = 12 Hz, CH$_2$), 9.3 (s, CH$_3$); ^{31}P{^{1}H} NMR (121.5 MHz, benzene-d$_6$): δ 11.9 (m, $J_{Rh,P}$ = 164.2 Hz, $J_{Rh,P}$ = 7.3 Hz, $J_{P,P}$ = 2.3 Hz), coupling constants were determined by simulation with gNMR[5]; IR (ATR): $\tilde{\nu}$ 978 (Rh=C=Rh) cm^{-1}; MS (LIFDI, Me$_6$Si$_2$): *m/z* 1008 [M]$^+$. Complex **7′** was prepared in a similar manner using ^{13}CS$_2$. Selected analytical data for *trans*-[Rh$_2$(μ-^{13}C)(SBpin)$_2$(PEt$_3$)$_4$] (**7′**): ^{31}P{^{1}H} NMR (121.5 MHz, benzene-d$_6$): δ 11.9 (m, $J_{Rh,P}$ = 164.2 Hz, $J_{C,P}$ = 11 Hz, $J_{Rh,P}$ = 7.3 Hz, $J_{P,P}$ = 2.3 Hz); IR (ATR): $\tilde{\nu}$ 946 (Rh=^{13}C=Rh) cm^{-1}.

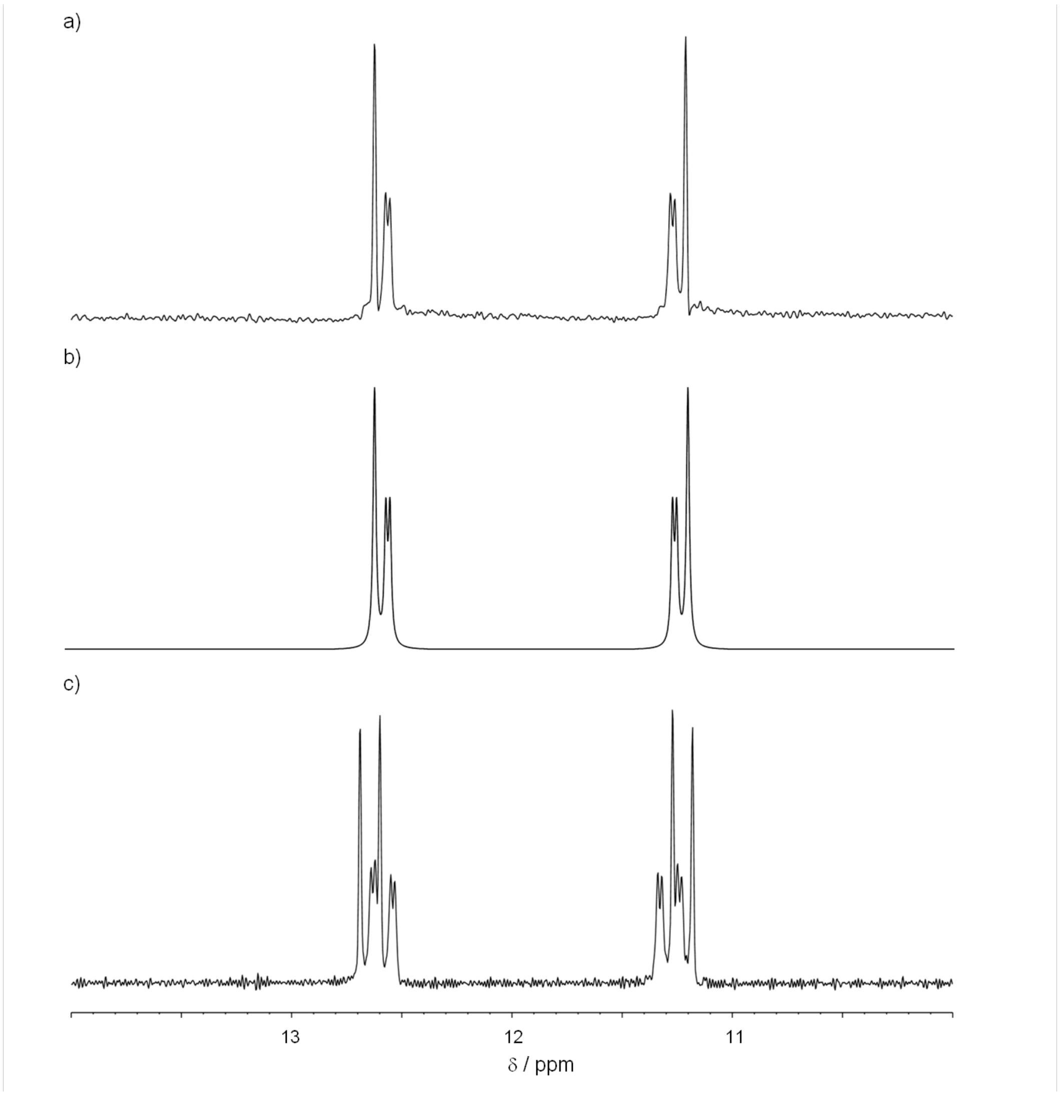

Figure S8. ^{31}P{^{1}H} NMR spectra (121.5 MHz, benzene-d$_6$) of **7** (a, observed; b, simulated) and **7′** (c, observed). The following coupling constants (Hz) were used for the simulation: $^2J_{Rh,P}$ = 164.2 Hz, $^4J_{Rh,P}$ = 7.3 Hz, $^5J_{P,P}$ = 2.3 Hz.

Orange crystals of *trans*-[$Rh_2(\mu\text{-}C)(SBpin)_2(PEt_3)_4$] (**7**) were grown at 0 °C from a methylcyclohexane solution.

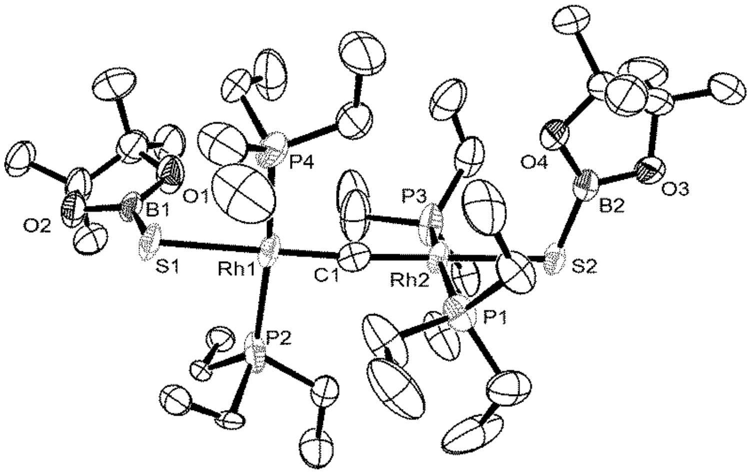

Figure S9. An ORTEP diagram of *trans*-[$Rh_2(\mu\text{-}C)(SBpin)_2(PEt_3)_4$] (**7**). The ellipsoids are drawn at the 50% probability level. The hydrogen atoms are omitted for clarity.

Table S4. Selected bond lengths (Å) and angles (°) for **7** with estimated standard deviations in parentheses

bond	length	bond	angle
C1-Rh1	1.790(7)	Rh2-C1-Rh1	176.1(4)
Rh2-C1	1.776(7)	C1-Rh2-P1	94.5(2)
Rh1-P2	2.332(2)	C1-Rh2-P3	92.8(2)
Rh1-P4	2.310(3)	P1-Rh2-P3	167.60(8)
Rh2-P1	2.322(2)	P2-Rh1-C1	93.1(2)
Rh2-P3	2.322(2)	P4-Rh1-C1	92.7(2)
Rh1-S1	2.4868(18)	P2-Rh1-P4	170.67(9)
Rh2-S2	2.4864(16)	C1-Rh2-S2	179.7(2)
S1-B1	1.777(10)	S1-Rh1-C1	179.7(2)
S2-B2	1.753(9)	P3-Rh2-S2	87.01(7)
B1-O1	1.379(10)	P1-Rh2-S2	85.63(7)
B1-O2	1.364(10)	Rh2-S2-B2	108.1(3)
B2-O3	1.388(10)	O3-B2-O4	110.8(7)
B2-O4	1.382(10)	O3-B2-S2	122.0(6)
		S2-B2-O4	127.3(6)

Treatment of *trans*-[Rh$_2$(μ-C)(SBpin)$_2$(PEt$_3$)$_4$] (6) with MeOH: Synthesis of *trans*-[Rh$_2$(μ-C)(SH)$_2$(PEt$_3$)$_4$] (8)

A solution of *trans*-[Rh$_2$(μ-C)(SBpin)$_2$(PEt$_3$)$_4$] (**7**) (20.1 mg, 20 μmol) in benzene (0.5 mL) was treated with MeOH (30 μL) and stirred for 1 d at room temperature. The volatiles were removed under vacuum and the residue was dissolved in *n*-hexane (0.2 mL). After cooling the solution to 203 K an orange solid precipitated, which was separated and washed with *n*-hexane (2 x 0.1 mL) at 203 K and dried in vacuum. Yield: 10 mg (66%). Analytical data for *trans*-[Rh$_2$(μ-C)(SH)$_2$(PEt$_3$)$_4$] (**8**): Anal. Calcd. (%) for $C_{25}H_{62}P_4Rh_2S_2\cdot 0.25$ *n*-hexane: C, 40.90; H, 8.48; S, 8.24. Found: C, 41.25; H, 8.49; S, 7.41; ^{1}H NMR (300.1 MHz, benzene-d$_6$): δ 2.03 (m, q in the ^{1}H{^{31}P} NMR spectrum, 24H, $J_{H,H}$ = 8 Hz, CH$_2$), 1.16 (m, t in the ^{1}H{^{31}P} NMR spectrum, 36H, $J_{H,H}$ = 8 Hz, CH$_3$), –2.09 (td, t in the ^{1}H{^{31}P} NMR spectrum, 2H, $J_{P,H}$ = 15 Hz, $J_{Rh,H}$ = 1 Hz, SH); ^{13}C{^{1}H} NMR (75.5 MHz, benzene-d$_6$): δ 431.9 (tquin, $J_{Rh,C}$ = 44 Hz, $J_{P,C}$ = 12 Hz, RhCRh), 17.6 (t, J = 13 Hz, CH$_2$), 9.0 (s, CH$_3$); ^{31}P{^{1}H} NMR (121.5 MHz, benzene-d$_6$): δ 11.9 (m, apparent couplings $J_{Rh,P}$ = 164 Hz, $J_{Rh,P}$ = 6 Hz); MS (LIFDI, Me$_6$Si$_2$): *m/z* 756 [M]$^+$, 638 [M-PEt$_3$]$^+$. Complex **8′** was prepared in a similar manner starting from **7′**. Selected analytical data for *trans*-[Rh$_2$(μ-^{13}C)(SH)$_2$(PEt$_3$)$_4$] (**8′**): ^{31}P{^{1}H} NMR (121.5 MHz, benzene-d$_6$): δ 11.8 (m, appartent couplings $J_{Rh,P}$ = 164 Hz, $J_{C,P}$ = 12 Hz, $J_{Rh,P}$ = 6 Hz).

The formation of MeOBpin and B(OMe)$_3$ as additional products was confirmed by ^{11}B{^{1}H} NMR spectroscopy and GC-MS analysis of the reaction solution.

Red crystals of *trans*-[Rh$_2$(μ-C)(SH)$_2$(PEt$_3$)$_4$] (**8**)·0.25 *n*-hexane were grown at –30 °C from a *n*-hexane solution. The X-ray diffraction data are of poor quality. Nevertheless the results support the suggested structure of **8**.

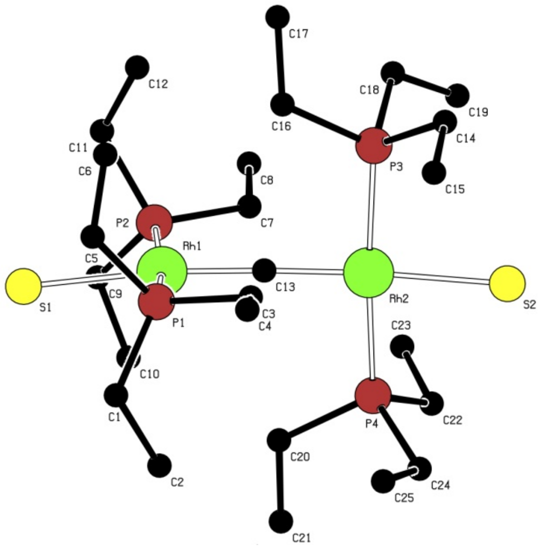

Figure S10. Structure of *trans*-[Rh$_2$(μ-C)(SH)$_2$(PEt$_3$)$_4$] (**8**).

Structure determination of the complexes 2·HOBpin, 4, 5, and 7

Crystals of **2·HOBpin**, **4**, and **5** precipitated from reaction solutions in *n*-hexane at –30 °C. Yellow crystals of **7** were grown at 0 °C from a methylcyclohexane solution. The diffraction data were collected on a STOE IPDS 2θ diffractometer at 100 K. Crystallographic data are depicted in Table S5. The structures were solved by direct methods (SHELXS-97)[6] and were refined with the full-matrix least-squares method on F^2 (SHELX-97 and SHELXL-2013)[7]. The hydrogen atoms were placed at the calculated positions and were refined by using a riding model.

Table S5. Crystallographic data

Compound	**2·HOBpin**	**4**	**5**	**7**
Empirical formula	$C_{19}H_{42}BO_4P_2Rh$, $C_6H_{13}BO_3$	$C_{24}H_{57}BO_3P_3Rh$	$C_{25}H_{47}BNO_3P_2Rh$	$C_{74}H_{176}B_4O_8P_8Rh_4S_4$, C_7H_{13}
Formula weight	654.16	600.32	585.30	2114.14
Crystal size (mm^3)	0.46 x 0.18 x 0.12	0.28 x 0.24 x 0.10	0.21 x 0.17 x 0.05	0.2 x 0.1 x 0.08
Wavelength (Å)	0.71073	0.71073	0.71073	0.71073
Crystal system	monoclinic	monoclinic	triclinic	monoclinic
space group	$P2_1$/n	$P2_1$	$P1$	$C2$/c
a (Å)	10.9348(7)	10.8214(8)	9.0037(11)	40.160(3)
b (Å)	25.1626(17)	13.3028(6)	11.2268(13)	15.9681(11)
c (Å)	12.1658(8)	11.7681(9)	15.1421(16)	20.1668(13)
α (°)			83.982(5)	
β (°)	93.209(2)	113.017(3)	80.950(4)	118.3330(18)
γ (°)			82.455(5)	
V (Å^3)	3342.1(4)	1559.21(18)	1492.9(3)	11383.2(13)
Z	4	2	2	4
Calculated density (Mg/m^3)	1.300	1.279	1.302	1.234
μ (Mo-K$_\alpha$) (mm^{-1})	0.643	0.723	0.703	0.798
θ range (°)	2.33 - 25.41	2.42 - 25.05	2.31 - 26.44	2.30 - 26.48
Reflections collected	92665	22344	30204	99844
Independent reflections	6154	5522	12047	11747
R$_{int}$	0.0401	0.0860	0.0605	0.1069
Goodness-of-fit on F^2	1.052	1.051	1.016	0.929
Completeness to max. θ	99.7%	99.9%	99.4%	99.7%
R$_1$, ωR$_2$ on all data	0.0243, 0.0606	0.0225, 0.0611	0.0669, 0.1218	0.1306, 0.2159
R$_1$, ωR$_2$ [$I_0>2\sigma(I_0)$]	0.0232, 0.0597	0.0224, 0.0611	0.0490, 0.1114	0.0689, 0.1728
Reflect. with [$I_0>2\sigma(I_0)$]	5917	5513	10115	7151
Largest diff. peak, hole (eA^{-3})	0.475/ -0.543	0.821/ -0.596	1.323/ -1.141	1.833/ -1.127
CCDC	1404746	1404747	1404748	1404749

DFT frequency mode analyses for 7 and 7´.

DFT frequency mode analyses for **7** and **7’** were performed using the atomic coordinates of **7** obtained by crystal structure analysis. The B3LYP functional was employed as implemented in the Gaussian09 program.[8,9] The C and H atoms of the peripheral ethyl groups were described by 6-31G* as standard basis sets, while the cc-ppVTZ-PP basis set was used for Rh atoms (including RECP). [10,11] All other atoms were described using cc-pVTZ basis sets.[12] A vibrational mode at $\tilde{\nu}$ 1021 cm^{-1} could be assigned to the metal carbide vibration of compound **7**. For the ^{13}C-isotopomer **7´** the metal carbide vibration was calculated to be found at a lower wavenumber ($\tilde{\nu}$ 987 cm^{-1}).

REFERENCES

1. M. Teltewskoi, J. A. Panetier, S. A. Macgregor, and T. Braun, *Angew. Chem. Int. Ed.*, 2010, **49**, 3947; *Angew. Chem.* **2010**, *122*, 4039.

2. M. Teltewskoi, S. I. Kalläne, T. Braun, and R. Herrmann, *Eur. J. Inorg. Chem.*, 2013, 5762.

3. J. K. MacDougall, M. C. Simpson, M. J. Green, and D. J. Cole-Hamilton, *J. Chem. Soc., Dalt. Trans.*, 1996, 1161.

4. S. I. Kalläne, T. Braun, B. Braun, and S. Mebs, *Dalton Trans.*, 2014, **43**, 6786.

5. P. H. M. Budzelaar, *gNMR*; Version 6.0, Ivory Software, 2006.

6. G. M. Sheldrick, *SHELXS-97*, Program for Crystal Structure Solution, University of Göttingen, 1997.

7. (a) G. M. Sheldrick, *SHELXL-97*, Program for Crystal Structure Refinement, University of Göttingen, 1997; (b) G. M.Sheldrick, *SHELXL2013*, Program for Crystal Structure Refinement, University of Göttingen, 2013.

8. (a) A. D. Becke, *J. Chem. Phys.*, 1993, **98**, 5648; (b) P. J. Stephens, F. J. Devlin, C. F. Chabalowski, M. J. Frisch, *J. Phys. Chem.*, 1994, **98**, 11623.

9. M. J. Frisch, G. W. Trucks, H. B. Schlegel, G. E. Scuseria, M. A. Robb, J. R. Cheeseman, G. Scalmani, V. Barone, B. Mennucci, G. A. Petersson, H. Nakatsuji, M. Caricato, X. Li, H. P. Hratchian, A. F. Izmaylov, J. Bloino, G. Zheng, J. L. Sonnenberg, M. Hada, M. Ehara, K. Toyota, R. Fukuda, J. Hasegawa, M. Ishida, T. Nakajima, Y. Honda, O. Kitao, H. Nakai, T. Vreven, J. A. Montgomery, Jr., J. E. Peralta, F. Ogliaro, M. Bearpark, J. J. Heyd, E. Brothers, K. N. Kudin, V. N. Staroverov, R. Kobayashi, J. Normand, K. Raghavachari, A. Rendell, J. C. Burant, S. S. Iyengar, J. Tomasi, M. Cossi, N. Rega, J. M. Millam, M. Klene, J. E. Knox, J. B. Cross, V. Bakken, C. Adamo, J. Jaramillo, R. Gomperts, R. E. Stratmann, O. Yazyev, A. J. Austin, R. Cammi, C. Pomelli, J. W. Ochterski, R. L. Martin, K. Morokuma, V. G. Zakrzewski, G. A. Voth, P. Salvador, J. J. Dannenberg, S. Dapprich, A. D. Daniels, Ö. Farkas, J. B. Foresman, J. V. Ortiz, J. Cioslowski, D. J. Fox, *Gaussian 09, Revision A.02*, Gaussian, Inc., Wallingford CT, 2009.

10. J. Hehre, R. Ditchfield, J. A. Pople, *J. Chem. Phys.*, 1972, **56**, 2257.

11. K. A. Peterson, D. Figgen, M. Dolg, H. Stoll, *J. Chem. Phys.*, 2007, **126**, 124101.

12. (a) T. H. Dunning, Jr., *J. Chem. Phys.*, 1989, **90**, 1007; (b) D. E. Woon T. H. Dunning, Jr., *J. Chem. Phys.*, 1993, **98**, 1358.